HHS Public Access

Author manuscript

Dent Mater. Author manuscript; available in PMC 2015 November 18.

Published in final edited form as:

Dent Mater. 2014 May ; 30(5): 564–569. doi:10.1016/j.dental.2014.02.019.

Characterization of a polymer-infiltrated ceramic-network material

Alvaro Della Bona[a], **Pedro H. Corazza**[b], and **Yu Zhang**[c]

[a]Post-graduation Program in Dentistry, Dental School, University of Passo Fundo, Passo Fundo, RS, Brazil

[b]Department of Dental Materials and Prosthodontics, Institute of Science and Technology of São José dos Campos, São Paulo State University (UNESP), São José dos Campos, SP, Brazil

[c]Department of Biomaterials & Biomimetics, College of Dentistry, New York University, New York, NY, USA

Abstract

Objectives—To characterize the microstructure and determine some mechanical properties of a polymer-ingfiltrated ceramic-network (PICN) material (Vita Enamic, Vita Zahnfabrik) available for CAD–CAM systems.

Methods—Specimens were fabricated to perform quantitative and qualitative analyses of the material's microstructure and to determine the fracture toughness (K_{Ic}), density (ρ), Poisson's ratio (v) and Young's modulus (E). K_{Ic} was determined using V-notched specimens and the short beam toughness method, where bar-shaped specimens were notched and 3-point loaded to fracture. ρ was calculated using Archimedes principle, and v and E were measured using an ultrasonic thickness gauge with a combination of a pulse generator and an oscilloscope.

Results—Microstructural analyses showed a ceramic- and a polymer-based interpenetrating network. Mean and standard deviation values for the properties evaluated were: K_{Ic} = 1.09 ± 0.05 MPa $m^{1/2}$, ρ = 2.09 ± 0.01 g/cm^3, v = 0.23 ± 0.002 and E = 37.95 ± 0.34 GPa.

Significance—The PICN material showed mechanical properties between porcelains and resin-based composites, reflecting its microstructural components.

Keywords

polymer-infiltrated ceramic-network; microstructure; short beam toughness; Young's modulus; Poisson's ratio

Introduction

Microstructural characterization and determination of the material properties are the first steps to understand the behavior of the materials used in restorative dentistry. Scanning electron microscopy (SEM) is a useful tool to provide information on topography [1–4] and

Correspondence to: Alvaro Della Bona.

microstructural parameters (stereology) such as particle size and shape [1, 3, 5]. When SEM is associated with energy dispersive spectroscopy (EDS), the information is enhanced by semi-quantitative chemical data of the material's phases. In addition, the density (ρ), the Young's modulus (*E*) and the Poisson's ratio (*v*) play an important role in the material's behavior [4], thereby are essential for finite element analysis [6, 7], which has increased in popularity in dental research. Nevertheless, the fracture toughness (K_{Ic}) has been reported as one of the key properties associated with the clinical performance of dental materials [8]. K_{Ic} indicates the ability of a material to resist crack propagation and, consequently, catastrophic failure. It has special relevance to fracture of brittle materials [9, 10]. For ceramic materials, the recommended method to determine K_{Ic} is the pre-crack-induced-test named single edge V-notched beam (SEVNB), which was found to be user friendly, repeatable, reliable and accurate, except for ceramics with pronounced R-curve behavior [11]. This method is based on notched bar-shaped specimens that are subsequently tested in flexure. The K_{Ic} value is calculated considering the failure load and the dimensions of the specimen and the notch. The notch design, specially the size of the notch root radius, affects the K_{Ic} value, so it is important to sharpen the notch until the root radius becomes approximately of the same size than the major microstructural feature size [12]. Yet, bar-shaped specimens fabricated from small size blocks, usually used for milling crowns in the CAD–CAM systems, present an additional challenge to determine the K_{Ic} value using V-notched specimens.

Ceramics and resin-based composites are the two main classes of dental restorative materials. Resin-based composites are composed of an organic polymer matrix and reinforcing inorganic filler particles [1, 13]. The amounts of filler particles are directly related to the Young's modulus and the hardness of the composites [1]. Development of filler technology has resulted in considerable improvements of the composites properties [1]. An important consideration to select the filler particles is the optical characteristic, and silica-based particles meet well this requirement [13]. On the other hand, the dimensional changes resulting from the polymerization are determined by the monomers of the polymer matrix, and the most common monomers are BisGMA, UDMA, UTMA, and Bis-EMA [13]. Nevertheless, the clinical performance of direct composites is still inferior to the performance of indirect ceramic restorations considering marginal adaptation, color match, and anatomic form [14]. A 3-year clinical study showed that indirect resin-based composite restorations have inferior esthetic and wear resistance compared to all-ceramic restorations [15]. Dental ceramics are essentially inorganic materials commonly composed of a crystalline phase and/or glass matrix [8]. Stronger and tougher ceramics, e.g. zirconia-based ceramics and alumina-based ceramics, have higher crystalline content and are more opaque than esthetic porcelains, e.g. silica-based ceramic [16]. However, the low K_{Ic} and high susceptibility to slow crack growth of the porcelains limit their clinical application [17].

Associating the Young's modulus of resin-based composites, which is similar to the dentin Young's modulus, with the long lasting esthetics of ceramics would be ideal for a restorative material. The newly developed polymer-infiltrated-ceramic-network (PICN) may offer an alternative solution. The fabrication process of this material requires two steps: first, a porous pre-sintered ceramic network is produced and conditioned by a coupling agent; second, this network is infiltrated with a polymer by capillary action [18]. The flexural

strength, elastic modulus, hardness and strain at failure of PICN structures were reported in a previous study [18], showing similar properties to the tooth structure and encouraging further studies on this material. Thus, the aim of the present study is to characterize the microstructure and determine some mechanical properties of a PICN material available for CAD–CAM systems, testing the hypothesis that the new material has properties ranging between porcelains and resin-based composites. In addition, this study applies the short beam toughness method to determine K_{Ic}.

Materials and methods

A PICN material (Vita Enamic, Vita Zahnfabrik, Bad Sackingen, Germany) was used to fabricate all specimens.

Microstructural characterization

Specimens were fabricated (n = 5) to perform quantitative and qualitative analyses of the microstructure. CAD–CAM blocks (17.5 mm × 14 mm × 12 mm) of the material were sectioned with a precision cutting machine (Isomet 1000, Buehler, Lake Bluff, USA), polished with metallographic papers (600, 800 and 1200-grit SiC) to the final dimension (2 mm × 14 mm × 12 mm) and finished with 1 μm alumina abrasive (Mark V Laboratory, East Granby, CT, USA). The specimens were sonically cleaned in acetone bath for 5 min, and then in isopropyl alcohol bath for additional 5 min before gold coated (SC7620 Sputter Coater, Quorum Technologies, Laughton, United Kingdom) and examined under the SEM (Jeol JSM-5310, Jeol, Japan) for the qualitative (SEI and BSI images) and quantitative (electron dispersive spectroscopy – EDS) analyses. Images in three different magnifications (1500×, 5000× and 20,000×) were recorded. Material composition, oxides and element concentrations (above 1 wt.%) were recorded from three different locations in each specimen using EDS. Average values were calculated.

Material properties

K_{Ic} was evaluated using the V-notched-beam test according to the ASTM C1421-10 standard [19]. Bar-shaped specimens (17.5 mm × 4 mm × 3 mm) were fabricated (n = 7) from CAD–CAM blocks using a precision cutting machine (Isomet 1000). The specimens were polished and positioned side-by-side on a flat holder, with the 3-mm wide face up, to be notched. The V-notch was created using a razor blade adapted in a notching machine (Equitecs, São Carlos, SP, Brazil). The machine applied a constant load of 10 kg on the razor blade, with a constant back-and-forth movement. A 6-μm diamond paste was used as an initial lubricant followed by a 1-μm diamond paste (Mipox Abrasives India, Bangalore, India). The final depth of the notch was approximately 1.1 mm. The specimens were removed from the holder and cleaned using alcohol in a sonic bath for 5 min. The notch root radius of each specimen was measured using SEM at 1000× magnification.

Specimens were positioned with the V-notched surface centered on the supporting rollers of a three-point flexure fixture and loaded to fracture using a universal testing machine (Emic DL-1000, Emic, Sao Jose dos Pinhais, PR, Brazil) with a crosshead speed of 0.5 mm/min. The distance (So) between the center of the rollers was 16 mm (Fig. 1). Therefore, the

specimens were 1.5 mm longer than the supporting span. As the width (*W*) of the specimen was 4 mm, the ratio *So/W* = 4.

The fractured specimens were prepared for SEM observation (100×), aiming for the measurement of the V-notch depth. Three readings of the notch depth per specimen were made (a_1, a_2 and a_3 – Fig. 2), and the average value (*a*) of the V-notch depth was calculated.

Relative V-notch depth (a) was obtained using the equation 1:

$$\alpha = \frac{a}{W} \quad (1)$$

The ratio *a/W* was approximately 0.3.

The K_{Ic} (MPa·$m^{0.5}$) was calculated following the precracked beam method (ASTM C1421-10 2010) (equations 2 and 3):

$$K_{Ic} = g\left[\frac{P_{max} S_0 10^{-6}}{B W^{3/2}}\right]\left[\frac{3[a/W]^{1/2}}{2[1-a/W]^{3/2}}\right] \quad (2)$$

Where

$$g = g\left(\frac{a}{W}\right) = \frac{1.99 - \left[\frac{a}{W}\right]\left[1-\frac{a}{W}\right]\left[2.15 - 3.93\left[\frac{a}{W}\right] + 2.7\left[\frac{a}{W}\right]^2\right]}{1+2\left[\frac{a}{W}\right]} \quad (3)$$

P_{max} is the load to failure (N) and B is the specimen thickness (m).

Specimens were prepared and polished, as described above, to evaluate the other material properties. Density (ρ) of the specimens was determined by the Archimedes principle, using an analytical balance (accuSeries II, Fischer Scientific, Pittsburgh, PA, USA) and the density kit accessory (Fischer Scientific). The weight of dry specimens (M_{dry}) and immersed in water (M_{fluid}) was obtained, and the bulk density was calculated using the following Eq. (4):

$$\rho = \frac{M_{dry}(\rho_{fluid} - \rho_{air})}{0.99983G} + \rho_{air} \quad (4)$$

where ρ_{fluid} was 0.99791 g/ml, the density of the water at experimental temperature conditions (21.5 °C); ρ_{air} was 0.0012 g/ml, the air density; and *G* is the buoyance (M_{dry} − M_{fluid}).

The material ratio (vol%) was estimated using stereology principles and Image J software. The thickness of the specimens was measured and used for *v* and *E* calculations. An ultrasonic gauge with a combination of a pulse generator and an oscilloscope (25DL Plus, Panametrics-NDT, Waltham, USA) was used. The velocity of longitudinal sound pulse (v_{long}) and shear (transverse) sound pulse (v_{shear}) were measured using longitudinal and

shear wave transducers attached to the specimens. *v* and *E* were calculated using the following Eqs. (5) and (6):

$$\nu = \frac{(v_{long}^2 - 2v_{shear}^2)}{2(v_{long}^2 - v_{shear}^2)} \quad (5)$$

$$E = \frac{\rho v_{long}^2 (1+v)(1-2v)}{1-v} \quad (6)$$

Results

Microstructural characterization

Representative images of the material microstructure (SEM–BSI) and a semi-quantitative EDS spectrum are shown in Fig. 3. Images showed a dominant (71 ± 3 vol%) ceramic network having leucite as the major phase and zirconia as a minor phase interconnected with a polymer-based network, which were confirmed by semi-quantitative EDS analyses. Few microcracks could be observed in the network boundaries.

The average values for the overall material composition (in wt.% of the present elements) and the oxides present in the ceramic network (in wt.%) were estimated using EDS analyses and they are presented in Table 1. Few other elements, such as Boron (B), calcium (Ca) and titanium (Ti), showed less than 1% and they were not reported. All phases were also independently analyzed using EDS, which showed mostly carbon (C) for the polymer-based network; silicon (Si), aluminum (Al), sodium (Na) and potassium (K) for the most predominant crystalline phase (* in Fig. 3B and C); and zirconium (Zr) for the other crystalline phase († in Fig. 3B and C).

Properties of the material

The notch root radius of the specimens ranged between 12 and 16 μm (Fig. 4).

The mean and standard deviation values for $K_{Ic}p$, *v* and *E* of the material are summarized in Table 2.

Discussion

This study characterized a new CAD–CAM material indicated for crowns, onlays/inlays, and veneers. The first report in the literature about this material [20] showed some promising mechanical properties, which were similar to enamel and dentin from human tooth, encouraging new studies. In the present study, the microstructural analyses suggested a hybrid material composed of interconnected networks: a dominant ceramic and a polymer. Compositional analyses of the dominant ceramic network revealed a major leucite-based phase of feldspar origin and a minor crystalline phase of zirconia, which could function as a strengthening component. Great amount of carbon was found on the polymer-based network, which the manufacturer (Vita Zahnfabrik) described as surface-modified PMMA (polymethyl methacrylate) free from MMA. Microstructurally, the ceramic network has

some resemblance of filler particles from resin-based composites [1, 13] and porcelains [3, 17].

High magnification microscopy showed few microcracks in the network boundaries. These defects can decrease the mechanical properties of materials [3].

Unsurprisingly, the mean values of the evaluated properties ranged between the values reported for resin-based composites and porcelains. The mean density value (2.09 ± 0.01 g/cm^3) is similar to mean values reported for a microhybrid composite (2.09 ± 0.01 g/cm^3) and for a nanofill composite (1.98 ± 0.003 g/cm^3) [1], slightly lower than the values reported for feldspathic porcelains (2.3–2.5 g/cm^3) [2], and much lower than the values reported for zirconia-reinforced, glass-infiltrated alumina-based ceramic (4.45 ± 0.01 g/cm^3) [4]. The mean *E* value (37.95 ± 0.34 GPa) is between the values reported for resin-based composites (21–25 GPa) [1] and feldspathic porcelains (66–67 GPa) [2]. Yet, it is slightly greater than the *E* values reported for a similar PICN material (28.1 GPa) [18], probably due to the presence of zirconia. Similarly, the mean *v* value (0.23 ± 0.002) is closer to the mean *v* values reported for porcelains (0.21–0.23) [2] than for resin-based composites (0.30–0.39) [21].

According to the manufacturer, the polymer–ceramic association significantly decreases the material's brittleness compared to porcelain. Fracture toughness (K_{Ic}) is a property related to the brittleness of the material and, again, the mean K_{Ic} value obtained for the evaluated material (1.09 ± 0.05 MPa m$^{1/2}$) is between porcelains (0.67–0.72 MPa m$^{1/2}$) [17] and resin-based composites (1.3–1.5 MPa m$^{1/2}$) used for direct restorations [1], but very close to the mean value of a highly filled (0.85 mass fraction spherical particles) resin-based composite (1.1 ± 0.2 MPa m$^{1/2}$) used different specimen and test configurations reported higher K_{Ic} values (1.46 and 1.8 MPa m$^{1/2}$) for similar PICN materials. The selection of the most convenient specimen geometry and fixture is governed by the objectives of the research and the microstructure and fracture behavior of the material of interest [8]. The critical notch root radius should be approximately of the same size than the major microstructural feature size for the SEVNB test, however, sometimes, it is impossible to produce such sharp notch [12]. Yet, the SEVNB is the test of choice to evaluate fracture toughness of ceramics [11], and it was previously used [25] to evaluate a very similar PICN material, which showed similar K_{Ic} value (1 ± 0.04 MPa m$^{1/2}$) to the present study (1.09 ± 0.05 MPa m$^{1/2}$). In the present study, the blocks from which the test specimens were fabricated only exist for milling crowns. Therefore, the specimens were shorter than the dimensions suggested in the standards (ISO 6872:2008 [11] and ASTM C1421-10 [19]). Thus, a polynominal solution (*g* factor in Eqs. (2) and (3)) was calculated based on previous studies [26–28].

The PICN material evaluated in the present study represents a fairly new concept for a dental material, associating features from both porcelains and resin-based composites. A similar concept was presented by Petrini et al. [29], where a biomimetic ceramic/polymer composite, consisting of a multi-level inorganic structure infiltrated with organic resin, has been developed and proposed for indirect restorations. The composite had different mechanical characteristics (Young's modulus, flexural strength and compressive strength) in different layers, reproducing the anisotropy of the tooth tissues. Both concepts seem

promising and should be further investigated. Yet, clinical trials are necessary to examine the behavior of such materials, allowing any comparison to existing restorative materials.

Conclusion

Characterization of the PICN material (Vita Enamic) revealed a leucite-based, zirconia-reinforced ceramic network interconnected with a polymer-based network, resulting in properties between porcelains and highly filled resin-based composites, confirming the study hypothesis.

Acknowledgement

The authors would like to thank Dr. George D. Quinn for the collaboration on the discussion of the manuscript. Supported by CNPq # 304995/2013-4 and the United States NIH/NIDCR 2R01 DE017925.

References

1. Rodrigues SA Jr, Scherrer SS, Ferracane JL, Della Bona A. Microstructural characterization and fracture behavior of a microhybrid and a nanofill composite. Dent Mater. 2008; 24:1281–1288. [PubMed: 18374408]
2. Borba M, de Araujo MD, de Lima E, Yoshimura HN, Cesar PF, Griggs JA, et al. Flexural strength and failure modes of layered ceramic structures. Dent Mater. 2011; 27:1259–1266. [PubMed: 21982199]
3. Della Bona A, Anusavice KJ. Microstructure, composition, and etching topography of dental ceramics. Int J Prosthodont. 2002; 15:159–167. [PubMed: 11951806]
4. Della Bona A, Donassollo TA, Demarco FF, Barrett AA, Mecholsky JJ Jr. Characterization and surface treatment effects on topography of a glass-infiltrated alumina/zirconia-reinforced ceramic. Dent Mater. 2007; 23:769–775. [PubMed: 17112579]
5. Sinmazisik G, Ovecoglu ML. Physical properties and microstructural characterization of dental porcelains mixed with distilled water and modeling liquid. Dent Mater. 2006; 22:735–745. [PubMed: 16324737]
6. Corazza PH, Feitosa SA, Borges AL, Della Bona A. Influence of convergence angle of tooth preparation on the fracture resistance of Y-TZP-based all-ceramic restorations. Dent Mater. 2013; 29:339–347. [PubMed: 23333235]
7. Geng JP, Tan KB, Liu GR. Application of finite element analysis in implant dentistry: a review of the literature. J Prosthet Dent. 2001; 85:585–598. [PubMed: 11404759]
8. Della Bona A. Bonding to ceramics: scientific evidences for clinical dentistry. São Paulo: Artes Médicas. 2009
9. Scherrer SS, Denry IL, Wiskott HW. Comparison of three fracture toughness testing techniques using a dental glass and a dental ceramic. Dent Mater. 1998; 14:246–255. [PubMed: 10379252]
10. Yilmaz H, Aydin C, Gul BE. Flexural strength and fracture toughness of dental core ceramics. J Prosthet Dent. 2007; 98:120–128. [PubMed: 17692593]
11. Dentistry - ceramic materials. 2008. ISO 6872.
12. Fischer H, Waindich A, Telle R. Influence of preparation of ceramic SEVNB specimens on fracture toughness testing results. Dent Mater. 2008; 24:618–622. [PubMed: 17709132]
13. Ferracane JL. Current trends in dental composites. Crit Rev Oral Biol Med. 1995; 6:302–318. [PubMed: 8664421]
14. Lange RT, Pfeiffer P. Clinical evaluation of ceramic inlays compared to composite restorations. Oper Dent. 2009; 34:263–272. [PubMed: 19544814]
15. Vanoorbeek S, Vandamme K, Lijnen I, Naert I. Computer-aided designed/computer-assisted manufactured composite resin versus ceramic single-tooth restorations: a 3-year clinical study. Int J Prosthodont. 2010; 23:223–230. [PubMed: 20552087]

16. Della Bona A, Kelly JR. The clinical success of all-ceramic restorations. J Am Dent Assoc. 2008; 139(Suppl.):8S–13S. [PubMed: 18768903]
17. Gonzaga CC, Yoshimura HN, Cesar PF, Miranda WG Jr. Subcritical crack growth in porcelains, glass-ceramics, and glass-infiltrated alumina composite for dental restorations. J Mater Sci Mater Med. 2009; 20:1017–1024. [PubMed: 19112607]
18. Coldea A, Swain MV, Thiel N. Mechanical properties of polymer-infiltrated-ceramic-network materials. Dent Mater. 2013; 29:419–426. [PubMed: 23410552]
19. Standard test methods for determination of fracture toughness of advanced ceramics at ambient temperature. 2010. ASTM C 1421-10.
20. He LH, Swain M. A novel polymer infiltrated ceramic dental material. Dent Mater. 2011; 27:527–534. [PubMed: 21371744]
21. Chung SM, Yap AU, Koh WK, Tsai KT, Lim CT. Measurement of Poisson's ratio of dental composite restorative materials. Biomaterials. 2004; 25:2455–2460. [PubMed: 14751729]
22. Quinn JB, Quinn GD. Material properties and fractography of an indirect dental resin composite. Dent Mater. 2010; 26:589–599. [PubMed: 20304478]
23. Fischer H, Marx R. Fracture toughness of dental ceramics: comparison of bending and indentation method. Dent Mater. 2002; 18:12–19. [PubMed: 11740960]
24. Nguyen JF, Ruse D, Phan AC, Sadoun MJ. High-temperature-pressure polymerized resin-infiltrated ceramic networks. J Dent Res. 2014; 93:62–67. [PubMed: 24186559]
25. Coldea A, Swain MV, Thiel N. In-vitro strength degradation of dental ceramics and novel PICN material by sharp indentation. J Mech Behav Biomed Mater. 2013; 26:34–42. [PubMed: 23807311]
26. Baratta FI, Fett T. Effect of load and crack misalignment on stress intensity factors for bend-type fracture toughness specimens. J Test Eval. 2000; 28:96–102.
27. Freese CE, Baratta FI. Single edge-crack stress intensity factor solutions. Eng Fracture Mech. 2006; 73:616–625.
28. Srawley JE. Wide range stress intensity factor expressions for ASTM E399 standard fracture toughness specimens. Int J Fracture Mech. 1976; 12:475–485.
29. Petrini M, Ferrante M, Su B. Fabrication and characterization of biomimetic ceramic/polymer composite materials for dental restoration.

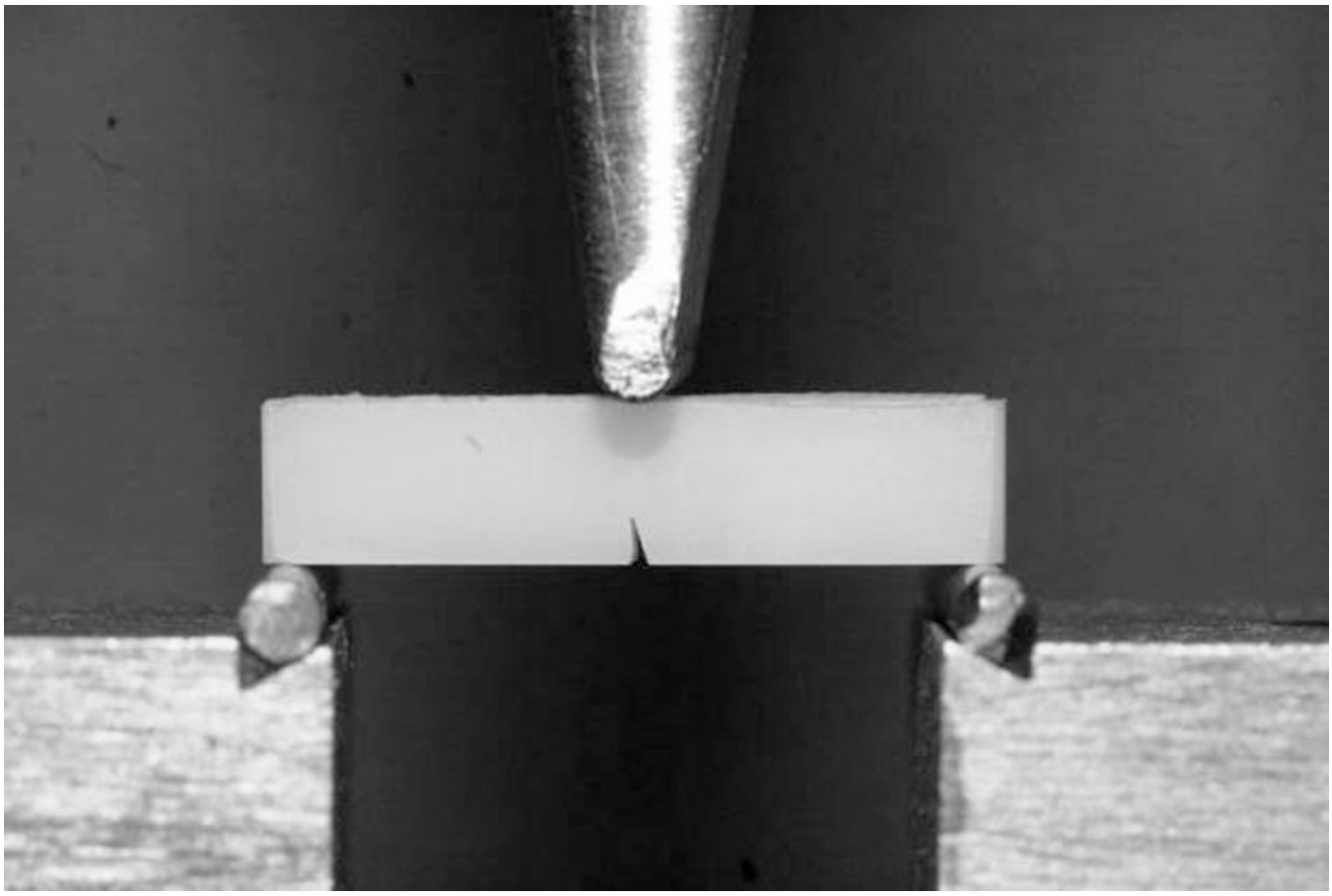

Figure 1.
Loaded V-notched specimen on a three point bending device Showing crack propagation.

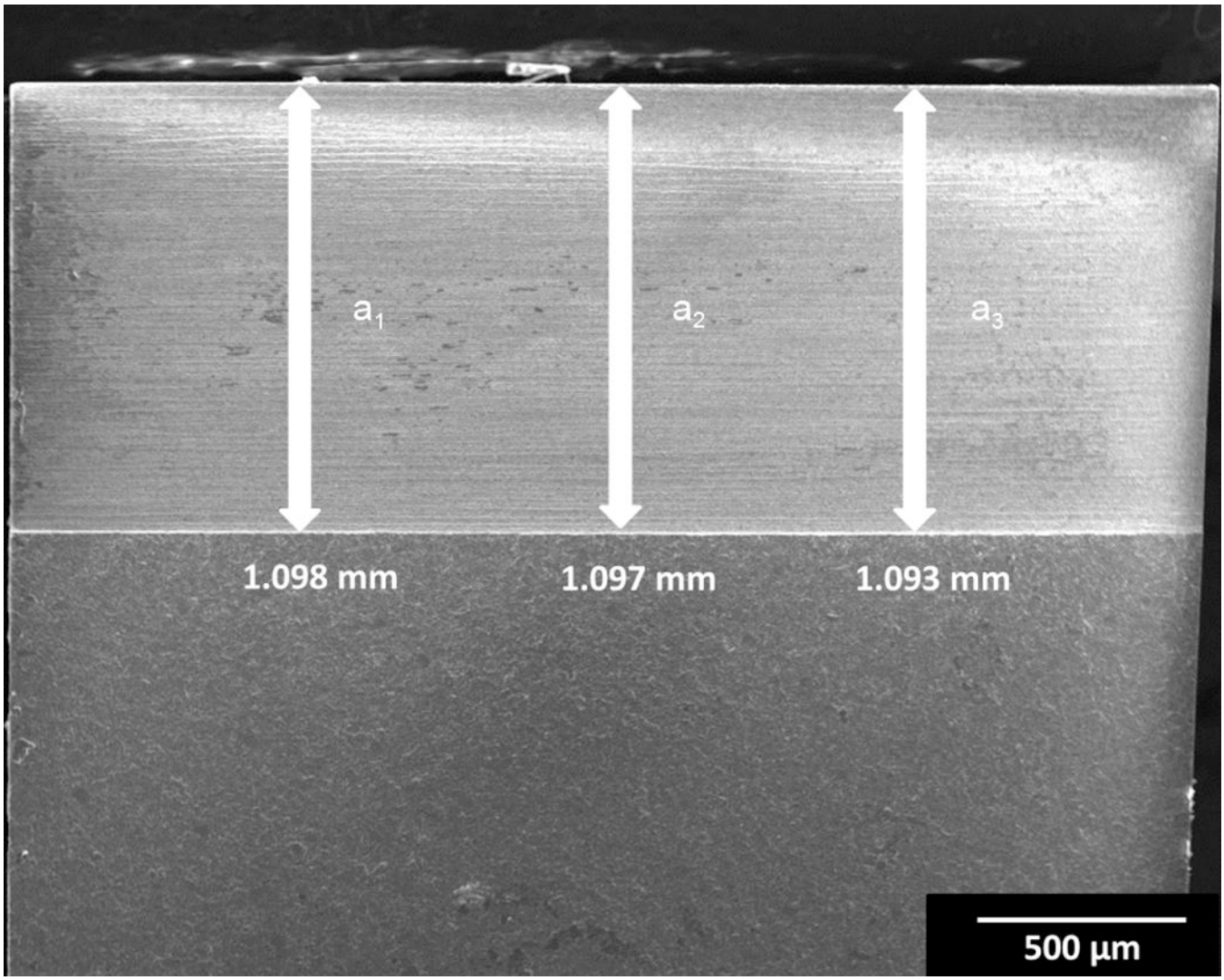

Figure 2.
V-notch depth (a) measurement using a SEM image (100×) of the specimen.

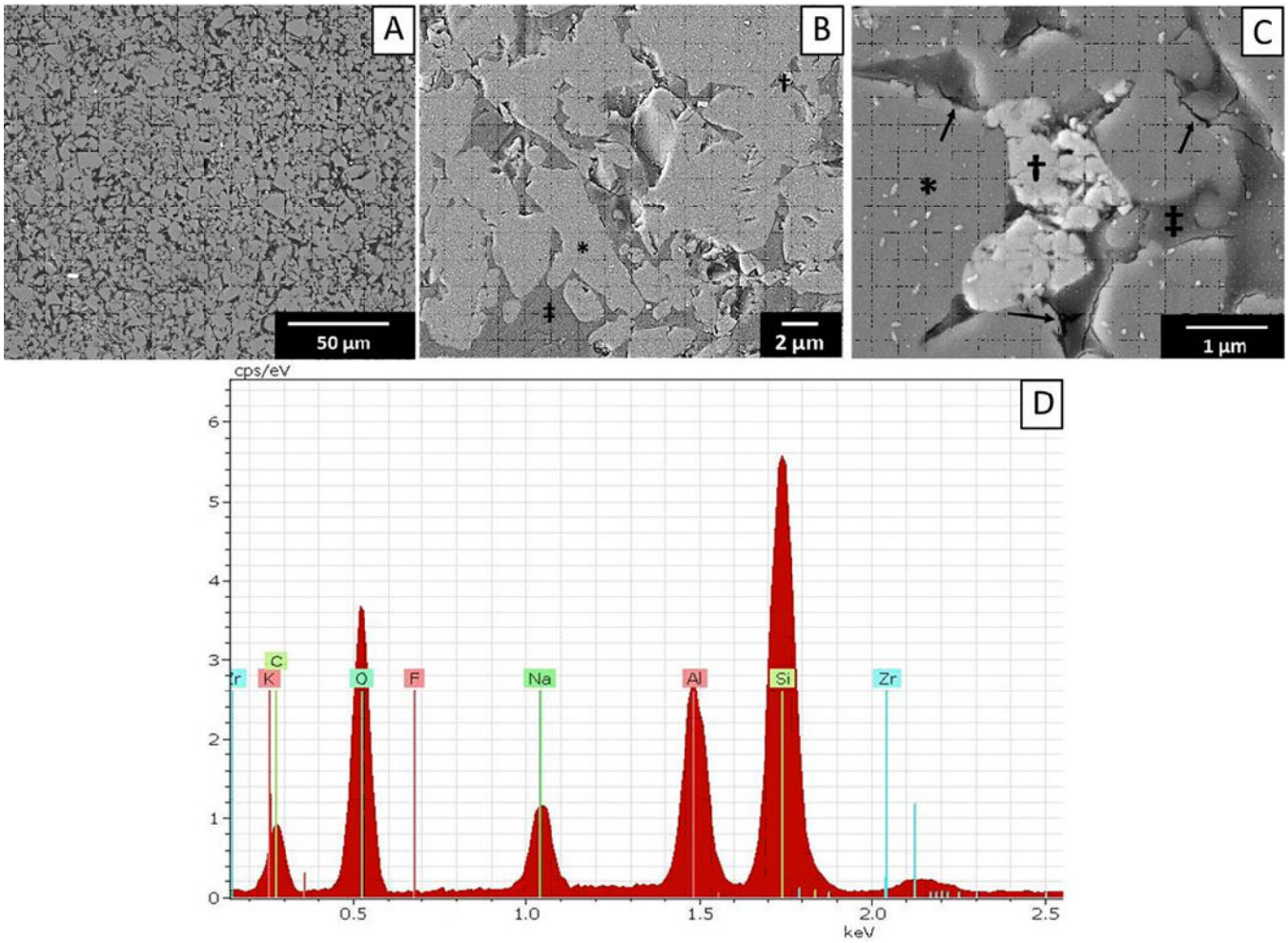

Figure 3.

(A–C) Representative micrographs (SEM–BSI) of the material microstructure and a semi-quantitative EDS spectrum (D) from (A). (A) Lower magnification (1500×) image shows two interconnected networks: a ceramic- and a polymer-based. (B and C) Close-up views (5000× and 20,000×) and EDS analyses identified the composition of the two-phase ceramic network as leucite (*) and zirconia (†) interconnected to a polymer-based network (‡). Few microcracks were observed in the network boundaries (black arrows).

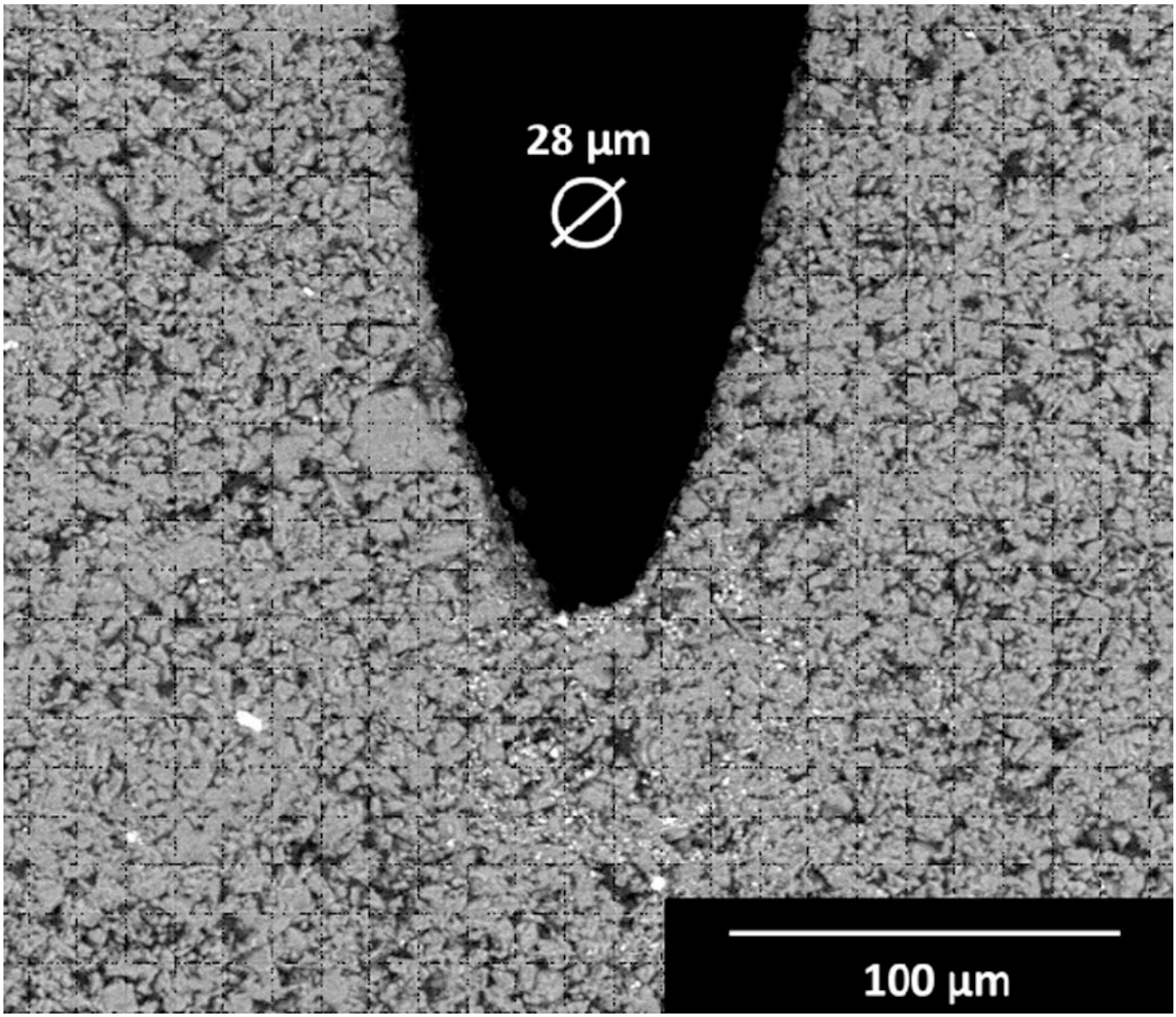

Figure 4.
SEM image showing a specimen notch with root diameter of 28 µm (or root radius of 14 µm) (1000×).

Table 1

Average values for the overall composition (elements) of the material and the oxides present in the ceramic network.

	Element (series)	wt%		Oxides	wt%
General elements	O(K)	44.5	**ceramic network**	SiO_2	54.9
	C(K)	23.4		Al_2O_3	24.8
	Si(K)	14.7		Na_2O	11.8
	Al(K)	8		K_2O	5.3
	Na(K)	5.6		ZrO_2	3.2
	K(K)	2.6			
	Zr(L)	1.2			

Table 2

Sample size (n) and mean and standard deviation (SD) values of fracture toughness (K_{IC}), density (ρ), Poisson's ratio (ν) and Young's modulus (*E*).

	K_{IC} (MPa·m$^{1/2}$)	**ρ (g/cm^3)**	**ν**	***E* (GPa)**
n	7	5	5	5
Mean (SD)	1.09 (0.05)	2.09 (0.01)	0.23 (0.002)	37.95 (0.34)